Figures and figure supplements

PTEN negatively regulates the cell lineage progression from NG2^{+} glial progenitor to oligodendrocyte via mTOR-independent signaling

Estibaliz González-Fernández *et al*

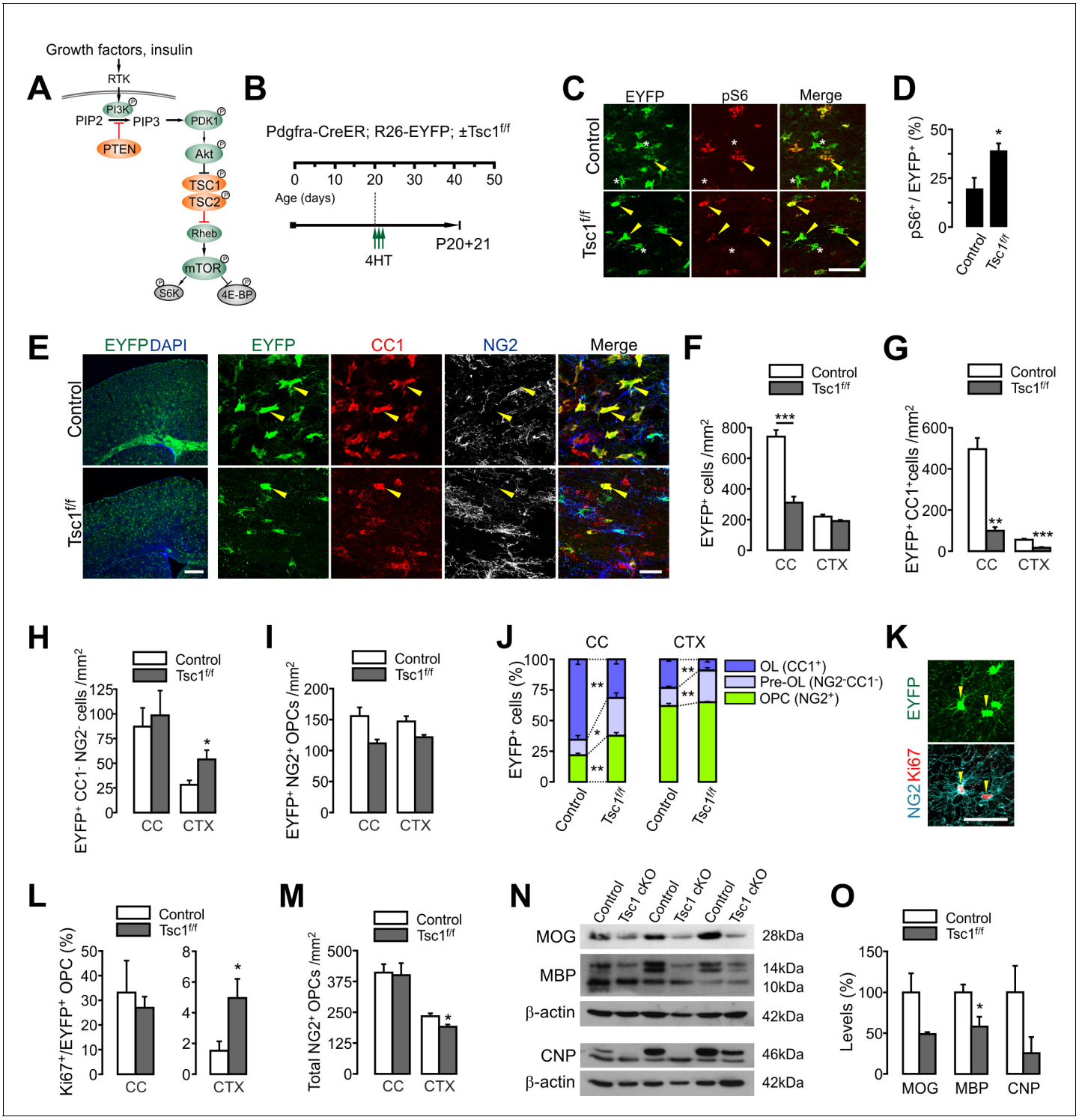

Figure 1. OPC-specific *Tsc1* ablation impairs oligodendrocyte development in the brain. (**A**) Schematic diagram of the Akt-mTOR signaling pathway. The TSC1/2 complex and PTEN (orange circles) negatively regulate mTOR activity, whereas other molecules in green circles positively regulate it. (**B**) Experimental scheme for 4HT administration into *Pdgfra-CreER; R26-EYFP; ±Tsc1$^{f/f}$* mice and mouse sampling. Three 4HT injections (1 mg per injection) were given between P20 and P21 (a total of 3 mg of 4HT). (**C**) Confocal images of phosphorylated S6 ribosomal protein (pS6) and EYFP$^+$ cells in the CC at P20 +21. Arrowheads and asterisks indicate EYFP$^+$ pS6$^+$ cells and EYFP$^+$ pS6$^-$ cells, respectively. Scale bar, 50 μm. (**D**) Quantification of the percentage of pS6$^+$ cells among EYFP$^+$ cells in the CC. n = 4 mice per group. (**E**) Fluorescence (left) and confocal microscopic (right) images of EYFP$^+$ cells in the control and *Tsc1* cKO mice (P20 +21). The confocal images of EYFP$^+$ cells were taken from the CTX, and show their maturation stages. Arrowheads indicate EYFP$^+$CC1$^+$ OLs. Scale bars, 500 μm (left) and 50 μm (right). (**F**) Quantification of EYFP$^+$ cells in the CC and CTX. (G - I) The

Figure 1 continued on next page

Figure 1 continued

numbers of EYFP$^+$CC1$^+$ OLs (**G**), EYFP$^+$CC1$^-$NG2$^-$ pre-OLs (**H**), and EYFP$^+$NG2$^+$ OPCs (**I**). (**J**) Percentages of OPC, pre-OL and OL among EYFP-labeled cells at P20 +21. n = 6 (control) or 3 (*Tsc1* cKO) mice for (F - J). (**K**) Cell proliferation analysis with Ki67-expressing patterns. Confocal images of EYFP$^+$NG2$^+$Ki67$^+$ OPCs in the CTX of a *Tsc1* cKO mouse. Scale bar, 50 μm. (**L**) The percentage of Ki67$^+$ cells among EYFP$^+$ OPCs. n = 4 mice per group. (**M**) The number of total OPCs. (**N**) Western blot analysis of cortical lysates (P20 +21) for myelin proteins MOG, MBP, and CNP. *Tsc1*$^{f/f}$ (control) and 4HT-administered *Pdgfra-CreER; Tsc1*$^{f/f}$ mice (*Tsc1* cKO) were used. (**O**) Quantification of levels of myelin proteins. n = 3 mice per group for (**N, O**). Data are represented as mean ±S.E.M. *p<0.05; **p<0.01; ***p<0.001. Unpaired Student's t-test. The numerical data for the graphs are available in ***Figure 1—source data 1***. Original western images are available in ***Figure 1—source data 2***.

DOI: https://doi.org/10.7554/eLife.32021.002

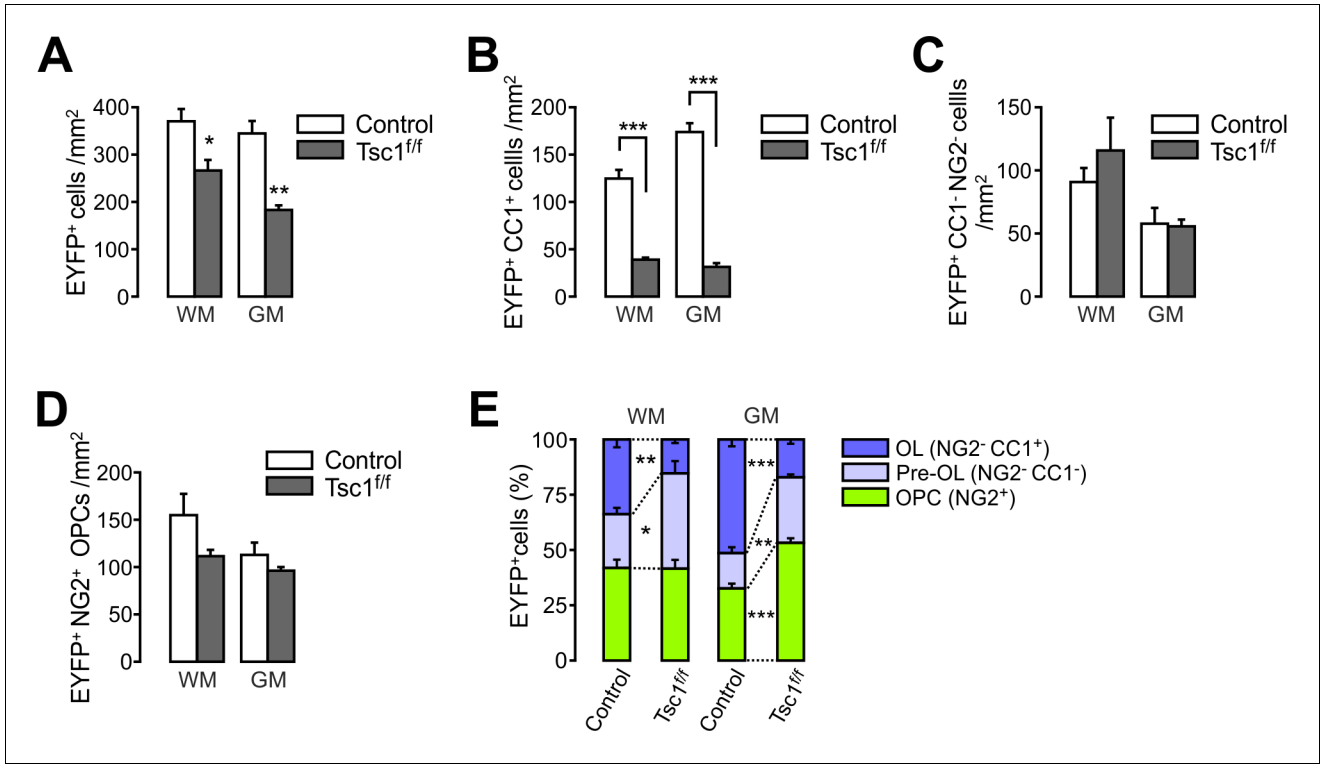

Figure 1—figure supplement 1. *Tsc1* deletion in OPCs impairs new oligodendrocyte development in the spinal cord. (**A**) The numbers of total EYFP$^+$ cells were reduced in the ventral spinal cord (SC) of *Pdgfra-CreER; R26-EYFP; Tsc1$^{f/f}$* (P20 +21) mice compared to their controls (*Pdgfra-CreER; R26-EYFP*). WM, white matter. GM, gray matter. (**B - D**) The number of EYFP$^+$CC1$^+$ OLs (**B**), EYFP$^+$CC1$^-$NG2$^-$ pre-OLs (**C**), and EYFP$^+$NG2$^+$ OPCs (**D**) in the SC. (**E**) Percentages of OPC, pre-OL, and OL among EYFP-labeled cells. Data are represented as mean ±S.E.M. n = 6 (control) or 3 (*Tsc1* cKO) mice. *p<0.05; **p<0.01; ***p<0.001. Unpaired Student's t-test. The numerical data for the graphs are available in ***Figure 1—figure supplement 1—source data 1***.

DOI: https://doi.org/10.7554/eLife.32021.003

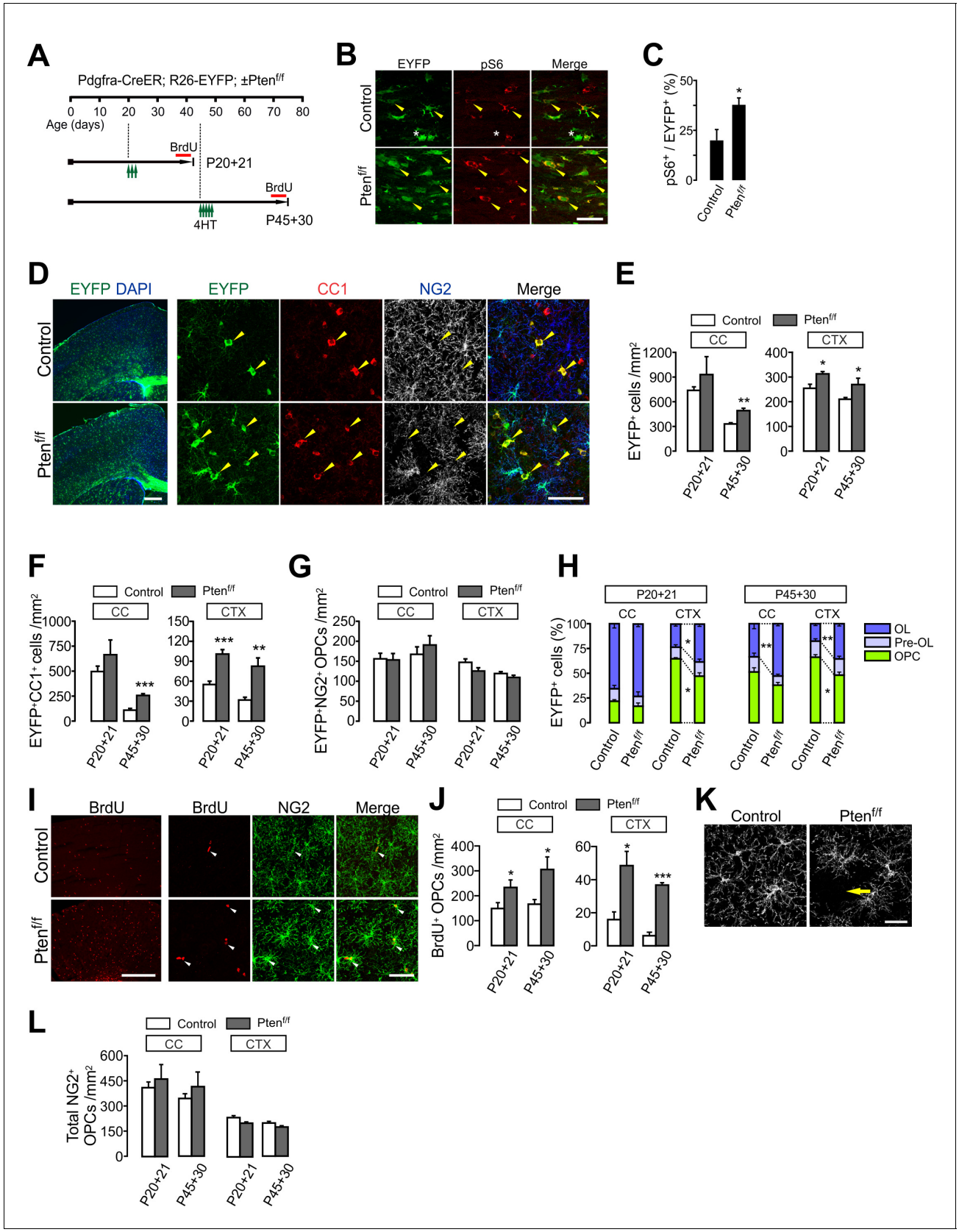

Figure 2. OPC-specific *Pten* ablation enhances oligodendrocyte differentiation and OPC proliferation in the brain. (**A**) Experimental scheme for 4HT injection and BrdU administration into *Pdgfra-CreER; R26-EYFP; ±Pten$^{f/f}$ mice*, and for mouse sampling. For P45 +30, 4HT (1 mg per injection) was

Figure 2 continued on next page

Figure 2 continued

injected five times between P45 and P47 (a total of 5 mg). (**B**) Confocal images of phosphorylated S6 ribosomal protein (pS6) and EYFP$^+$ cells in the CC at P20 +21. Arrowheads and asterisks indicate EYFP$^+$ pS6$^+$ cells and EYFP$^+$pS6$^-$ cells, respectively. Scale bar, 50 μm. (**C**) Percentage of pS6$^+$ cells among EYFP-labeled cells in the CC at P20 +21. n = 5 mice per group. (**D**) Fluorescence (left) and confocal (right) images of EYFP$^+$ cells in the brains of the 4HT-administered control and *Pten* cKO mice (P20 +21). The confocal images were taken from the CTX. Arrowheads indicate EYFP$^+$CC1$^+$ mature OLs. Scale bars, 500 μm (left) and 50 μm (right). (**E**) Number of total EYFP$^+$ cells was increased in the CTX of *Pten* cKO mice during the OPC fate analysis for the two age windows. (**F**) Number of EYFP$^+$CC1$^+$ OLs. (**G**) The numbers of EYFP$^+$NG2$^+$ OPCs were not changed by the *Pten* cKO. (**H**) Percentages of OPC, pre-OL and OL among EYFP-labeled cells. (**I**) Fluorescence (left) and confocal (right) images of BrdU$^+$ cells in the CTX (P20 +21). Arrowheads indicate BrdU$^+$NG2$^+$ OPCs. Scale bars, 500 μm (left) or 50 μm (right). (**J**) Quantification of BrdU$^+$NG2$^+$ OPCs in the CC and CTX. (**K**) Confocal images showing disruption of tiled OPC distribution in the CTX of *Pten* cKO mice (P20 +21). An arrow indicates a cortical area devoid of an NG2$^+$ OPC. Scale bar, 50 μm. (**L**) Number of total OPCs. Data are represented as mean ±S.E.M. n = 4 ~ 7 mice per group for P20 ~41. n = 3 ~ 5 mice per group for P45 ~P75. *p<0.05; **p<0.01; ***p<0.001. Unpaired Student's t-test. The numerical data for the graphs are available in ***Figure 2—source data 1***.

DOI: https://doi.org/10.7554/eLife.32021.007

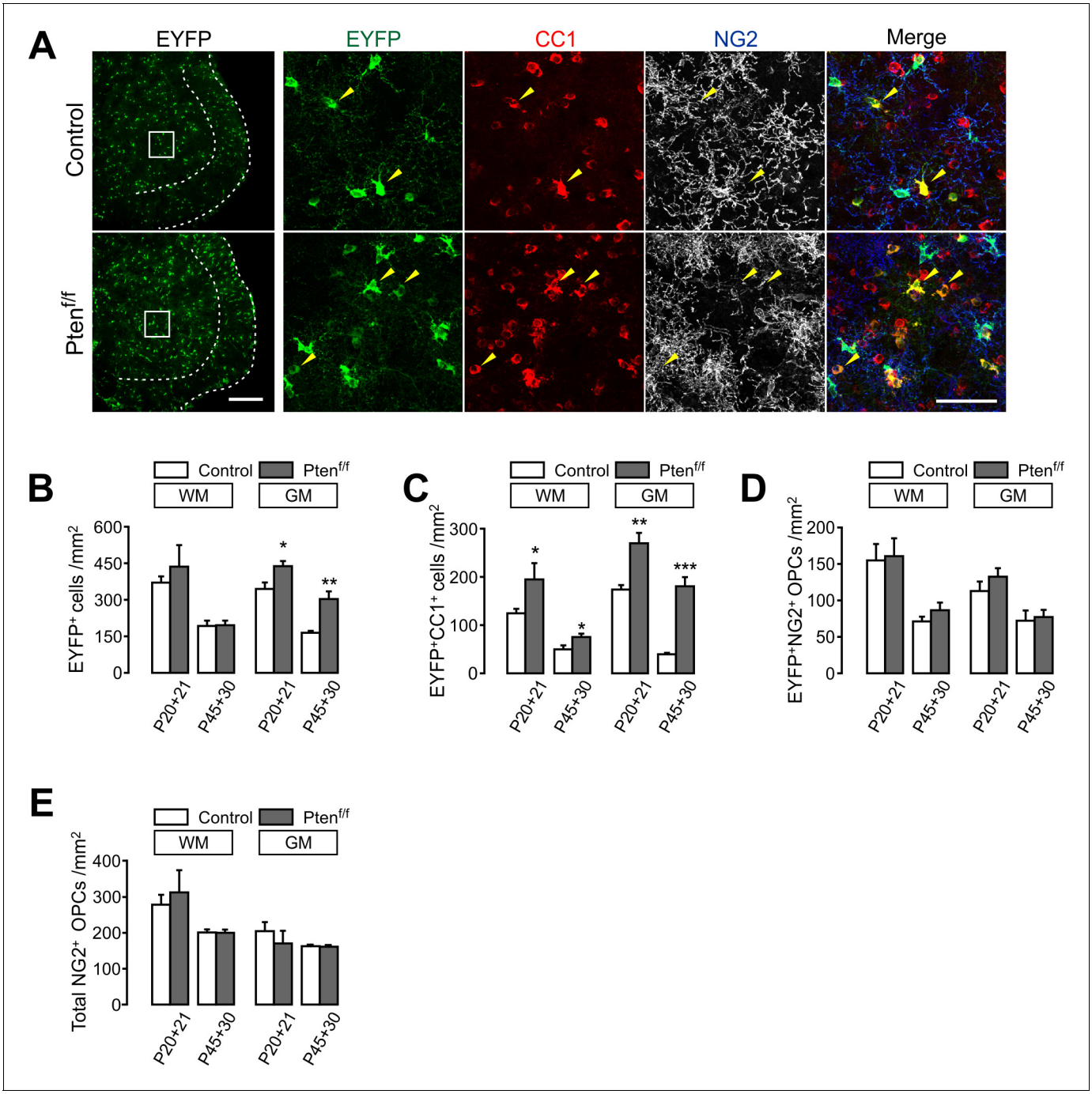

Figure 2—figure supplement 1. OPC-specific *Pten* ablation enhances oligodendrocyte differentiation in the spinal cord. (**A**) Fluorescence (left) and confocal (right) images of SC EYFP$^+$ cells in *Pdgfra-CreER; R26-EYFP;* ±*Pten*$^{f/f}$ mice (P20 +21). The identity of EYFP$^+$ cells in the boxed areas (left) was determined by co-immunostaining with maturation stage markers (right). Arrowheads indicate newly generated EYFP$^+$CC1$^+$ OLs. Scale bars, 100 µm (left) and 50 µm (right). (B - E) Quantification of EYFP$^+$ cells (**B**), EYFP$^+$CC1$^+$ new OLs (**C**), EYFP$^+$NG2$^+$ OPCs (**D**) and total NG2$^+$ OPCs (**E**) in the SC of control and *Pten* cKO mice. Data are represented as mean ±S.E.M. n = 3 ~ 6 (control), or 3 ~ 5 (*Pten* cKO) mice. *p<0.05; **p<0.01; ***p<0.001. Unpaired Student's t-test. The numerical data for the graphs are available in ***Figure 2—figure supplement 1—source data 1***.

DOI: https://doi.org/10.7554/eLife.32021.008

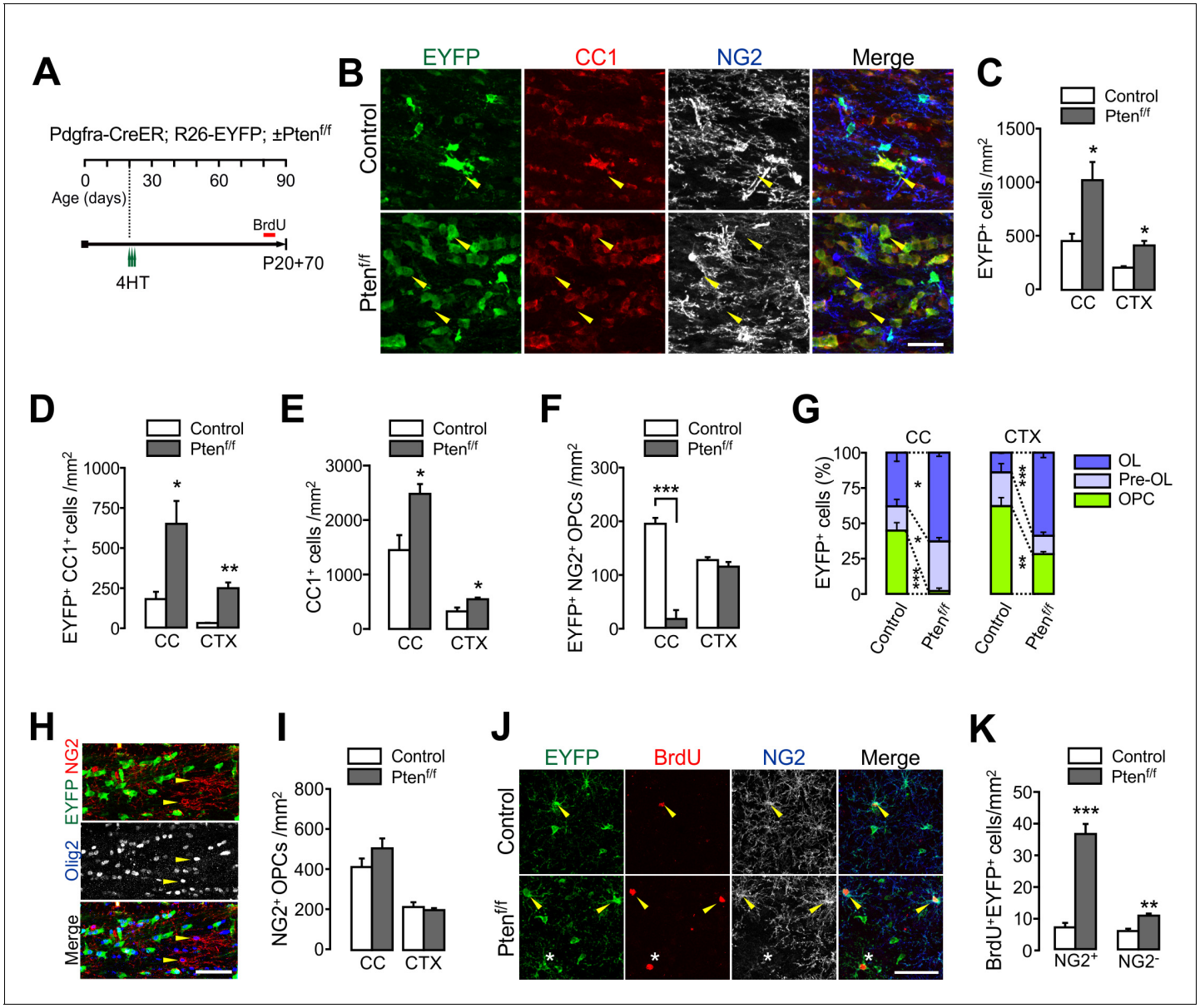

Figure 3. PTEN-deficient OPCs continuously add new oligodendrocytes. (**A**) Experimental scheme for 4HT and BrdU administration into *Pdgfra-CreER; R26-EYFP; ±Pten$^{f/f}$* mice, and for mouse sampling at P90 (P20 +70). (**B**) Confocal images of EYFP$^+$ cells in the CC showing their maturation stage. Arrowheads indicate EYFP$^+$CC1$^+$ OLs. Scale bar, 50 µm. (**C**) Number of EYFP$^+$ cells in the CC and CTX at P20 +70. (**D**) Number of EYFP$^+$CC1$^+$ OLs. (**E**) Number of total CC1$^+$ OLs. (**F**) Number of EYFP$^+$NG2$^+$ OPCs. (**G**) Percentages of OPC, pre-OL and OL among EYFP-labeled cells in the control and *Pten* cKO mice at P20 +70. (**H**) Confocal images of NG2$^+$ OPCs in the CC of *Pten* cKO mice. At P20 +70, resident Olig2$^+$NG2$^+$ OPCs did not EYFP$^+$ OPCs (arrowheads) in the CC. Scale bar, 50 µm. (**I**) The number of total NG2$^+$ OPCs did not change in *Pten* cKO mice. (**J**) Confocal images of cortical EYFP-labeled BrdU$^+$ cells. Arrowheads and asterisk indicate BrdU$^+$NG2$^+$ OPCs and a BrdU$^+$NG2$^-$ cell, respectively. (**K**) Number of BrdU$^+$EYFP$^+$NG2$^+$ OPCs and BrdU$^+$EYFP$^+$NG2$^-$ OL lineage cells in the CTX. Data are represented as mean ±S.E.M. n = 3 (control) and 4 (*Pten* cKO) mice. *p<0.05; **p<0.01; ***p<0.001. Unpaired Student's t-test. The numerical data for the graphs are available in ***Figure 3—source data 1***.

DOI: https://doi.org/10.7554/eLife.32021.011

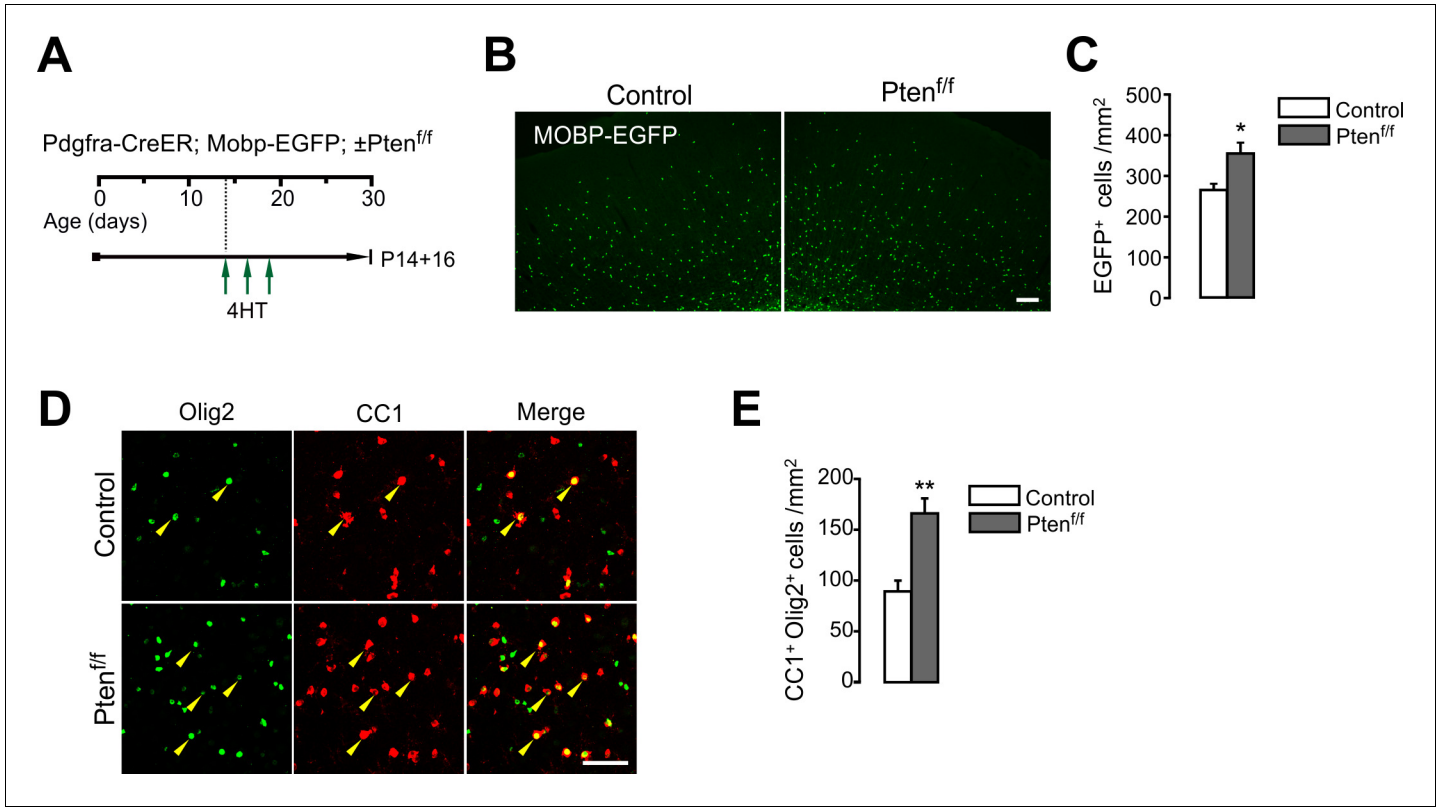

Figure 3—figure supplement 1. OPC-specific *Pten* ablation facilitates oligodendrocyte accumulation in the cortex. (**A**) The experimental scheme for 4HT administration into *Pdgfra-CreER; Mobp-EGFP; ±Pten*$^{f/f}$ mice and mouse sampling (P14 +16). 4HT was injected at P14, 16 and 18 (one single injection per day). (**B**) Fluorescence images of EGFP^{+} cells in the CTX. Scale bar, 100 µm. (**C**) Quantification of EGFP^{+} OLs in the CTX at P14 +16. (**D**) Confocal images of cortical Olig2^{+}CC1^{+} OLs (arrowheads). Some CC1^{+} (or EGFP^{+}) OLs were not labeled with our Olig2 immunostaining. Scale bar, 50 µm. (**E**) Quantification of Olig2^{+}CC1^{+} OLs in the CTX at P14 +16. Data are represented as mean ±S.E.M. n = 4 (control) or 3 (*Pten* cKO) mice. *p<0.05; **p<0.01. Unpaired Student's t-test. The numerical data for the graphs are available in ***Figure 3—figure supplement 1—source data 1***.

DOI: https://doi.org/10.7554/eLife.32021.012

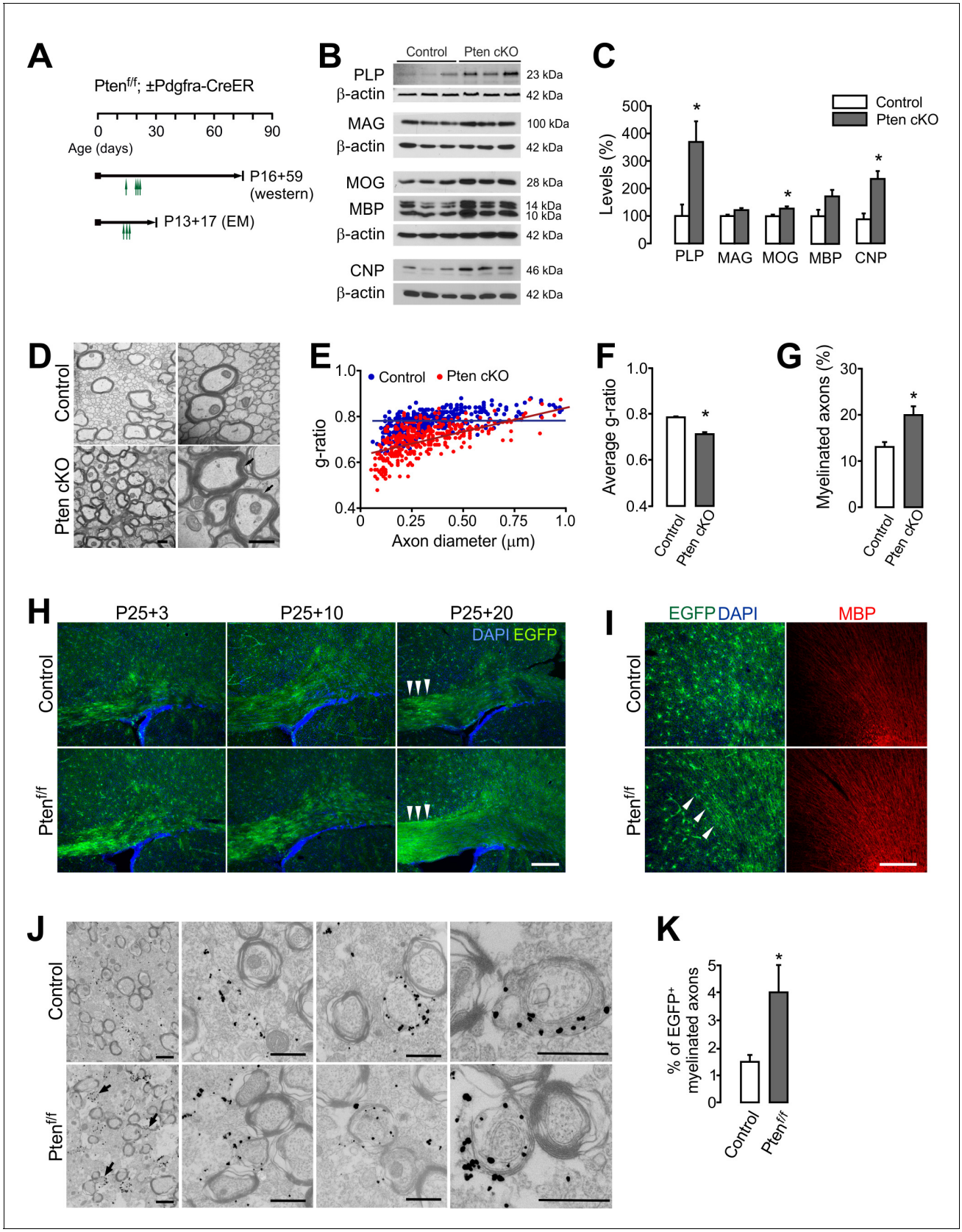

Figure 4. OPC-specific *Pten* ablation promotes new myelination. (**A**) Experimental scheme for 4HT into *Pten*$^{f/f}$ ± *Pdgfra-CreER* mice, and for mouse sampling for western blot analysis (**B,C**) and EM analyses (D –G). For western blot analysis, 4HT was injected into *Pten*$^{f/f}$ (control) and *Pdgfra-CreER;*

Figure 4 continued on next page

Figure 4 continued

Pten$^{f/f}$ mice at P14, P20 (twice), and P21 (1 mg per injection, a total of 4 mg), and the mice were sampled at P75. For EM, A single dose 4HT was injected at P13, 15, and 17 (a total of 3 mg), and the mice were sampled at P30. (**B**) Western blot analysis of cortical lysates for myelin proteins of control and OPC-targeted *Pten* cKO mice (P14 +61). (**C**) Quantification of the levels of PLP, MAG, MOG, MBP and CNP in the western blot (**B**). n = 3 mice per group. (**D**) Representative electron micrograph (EM) of the CC of the control and *Pten* cKO mice (P13 +17). Arrows indicate thickened myelin in *Pten* cKO mice. Scale bar, 500 nm. (**E**) Scatter plot of g-ratios. More than 100 myelinated axons per mouse were analyzed. (**F**) Average g-ratio. (**G**) Percentage of myelinated axons was increased in *Pten* cKO mice. More than 700 axons were analyzed for myelination per mouse. n = 3 mice per group for (D - G). (**H, I**) Fluorescence images of EGFP^{+} cells in the CC (**G**) and CTX (**H**) of *Pdgfra-CreER; R26-mEGFP;±Pten*$^{f/f}$ mice. 4HT (1 mg per injection, two injections per day) was injected at P25 and P26 (a total of 4 mg), and the mice were killed 3, 10, or 20 days later. Arrowheads indicate increased EGFP^{+} slender processes, reminiscent of bundles of myelinated fibers in *Pten* cKO mice (P25 +20). Scale bar, 100 μm. (**J**) Immuno-EM of anti-EGFP immuno-gold particles in the CC of *Pdgfra-CreER; R26-mEGFP; ±Pten*$^{f/f}$ mice (P20 +21). Arrows indicate EGFP^{+} newly formed immature myelin sheaths. Scale bar, 500 nm. (**K**) Percentage of EGFP^{+} myelinated axons increased at P20 +21. n = 3 mice per group. Data are represented as mean ±S.E.M. *p<0.05. Unpaired Student's t-test. The numerical data for the graphs are available in ***Figure 4—source data 1***. Original western images are available in ***Figure 4—source data 2***.

DOI: https://doi.org/10.7554/eLife.32021.015

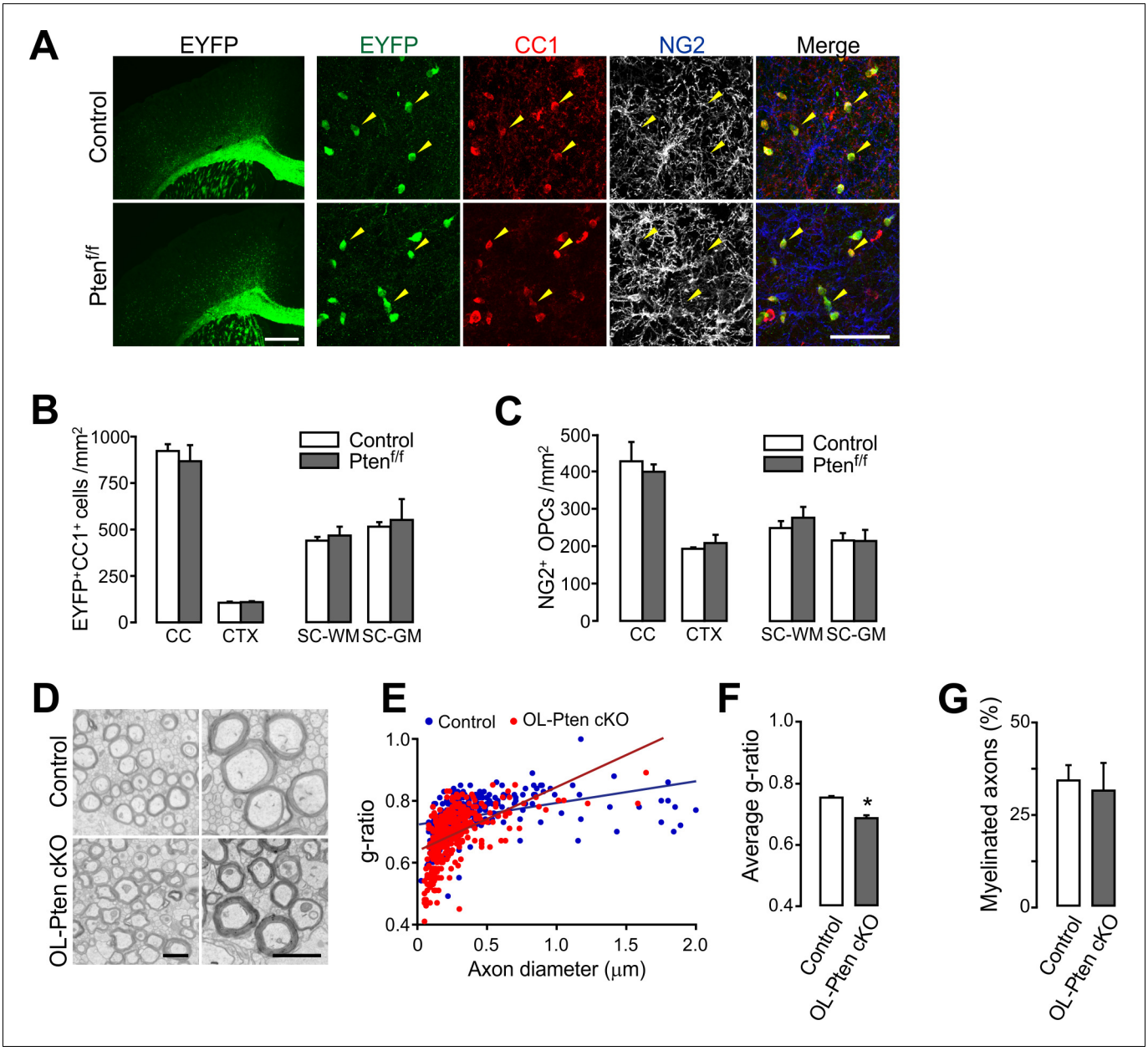

Figure 5. Oligodendrocyte numbers and the degree of new myelination are not changed by OL-specific *Pten* ablation. (**A**) Fluorescence (left) and confocal (right) images of EYFP$^+$ cells in *Mog-iCre; R26-EYFP; ±Pten$^{f/f}$* (**P41**) mice. The confocal images were taken from the CTX. Arrowheads indicate EYFP$^+$CC1$^+$ OLs. Scale bars, 500 μm (left) and 50 (right) μm. (**B**) Number of EYFP$^+$CC1$^+$ OLs in the brain and the SC. (**C**) Number of NG2$^+$ OPCs. (**D**) Representative EM of myelinated callosal axons from *R26-EYFP; Pten$^{f/f}$* (control) and *R26-EYFP; Pten$^{f/f}$; ±Mog-iCre* (*Pten* cKO) mice (**P34**). Scale bar, 500 nm. (**E**) Scatter plot of the g-ratios. More than 100 axons per mouse, and three mice per group were analyzed. (**F**) Average g-ratio. (**G**) Percentage of myelinated axons was not altered in OL-specific *Pten* cKO mice. Data are represented as mean ±S.E.M. n = 3 (control) or 4 (*Pten* cKO) mice for (**B, C**), and n = 3 mice per group for (D - G). *p<0.05. Unpaired Student's t-test. The numerical data for the graphs are available in ***Figure 5—source data 1***.
DOI: https://doi.org/10.7554/eLife.32021.018

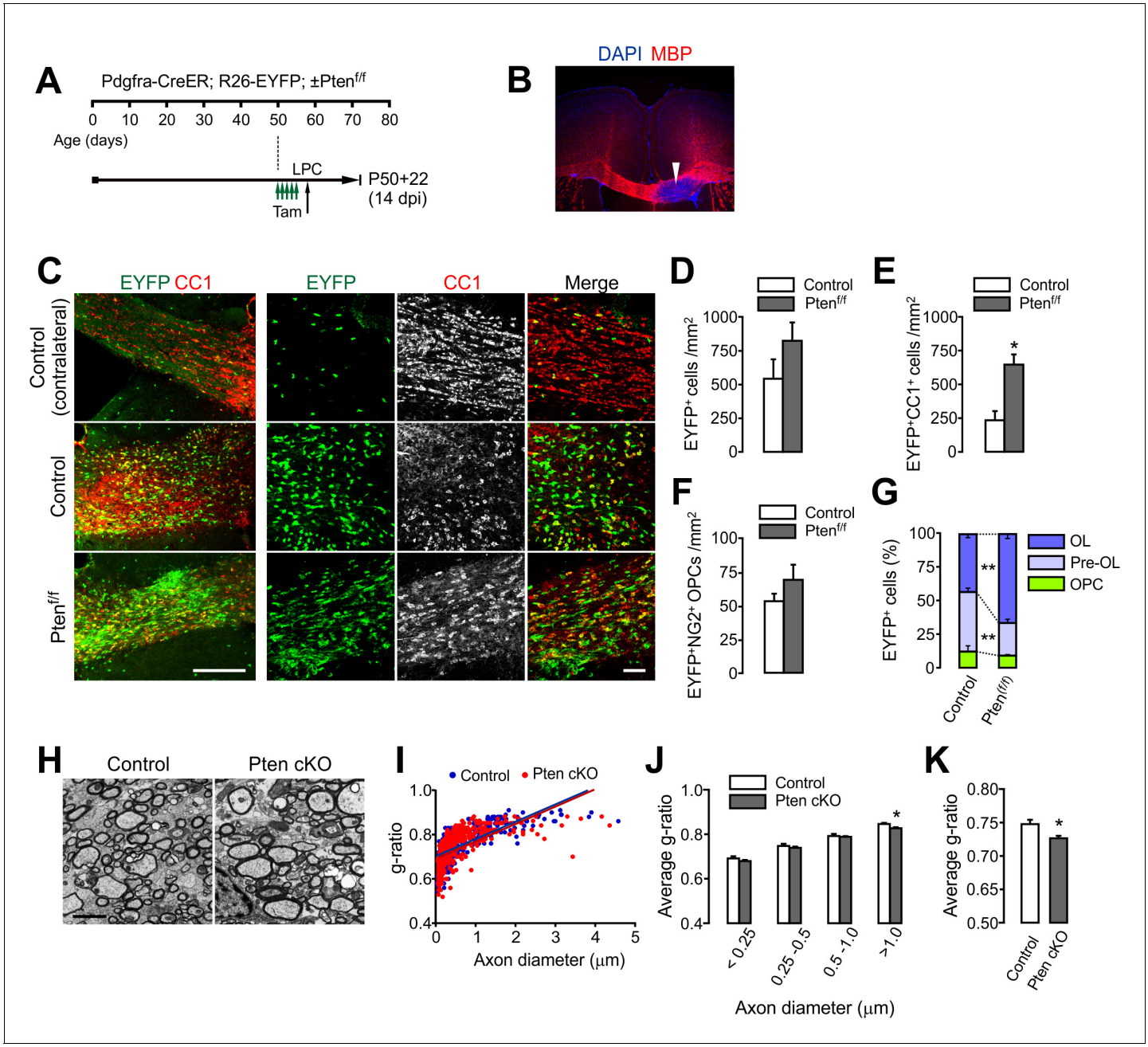

Figure 6. OPC-specific *Pten* ablation facilitates oligodendrocyte regeneration and remyelination after LPC-induced demyelination. (**A**) Experimental scheme for tamoxifen (Tam) and lysolecithin (LPC) injection into *Pdgfra-CreER; R26-EYFP; ±Pten$^{f/f}$* mice. A series of tamoxifen injections (40 mg/kg per i.p. injection, a total of 10 injections) were given between P50 and P54. The demyelination was induced with LPC injection at P58, and the mice were sampled at P72, which is 14 days after LPC injection (14 dpi), and 22 days after the first tamoxifen injection (P50 +22). (**B**) Loss of MBP immunoreactivity (arrowhead) at the LPC-injected CC in the brain. (**C**) Fluorescence (left) and confocal (right) images of EYFP$^+$ cells and CC1$^+$ OLs in the CC at 14 days after LPC injection (14 dpi). Scale bars, 200 μm (left) and 50 μm (right). (**D**) Quantification of EYFP$^+$ cells in the LPC injected site at 14 dpi. (**E**) Quantification of EYFP$^+$CC1$^+$ OLs. (**F**) Quantification of EYFP$^+$NG2$^+$ OPCs. (**G**) *Pten* cKO mice exhibited marked changes in the percentage of OL and pre-OL among EYFP-labeled cells at the LPC-injected areas at 14 dpi. (**H**) Representative EMs of the lesion in the CC at 14 dpi. Scale bar, 2 μm. (**I**) Scatter plot for individual g-ratios of myelinated axons. More than 100 myelinated axons per mouse, and three mice per group were analyzed. (**J, K**) Average g-ratio according to axon diameter (**J**) and as a total (**K**). Data are represented as mean ±S.E.M. n = 3 (control) or 5 (*Pten* cKO) mice for (D - G), or n = 3 per group for (**H–K**). *p<0.05; **p<0.01. Unpaired Student's t-test. The numerical data for the graphs are available in ***Figure 6—source data 1***.
DOI: https://doi.org/10.7554/eLife.32021.020

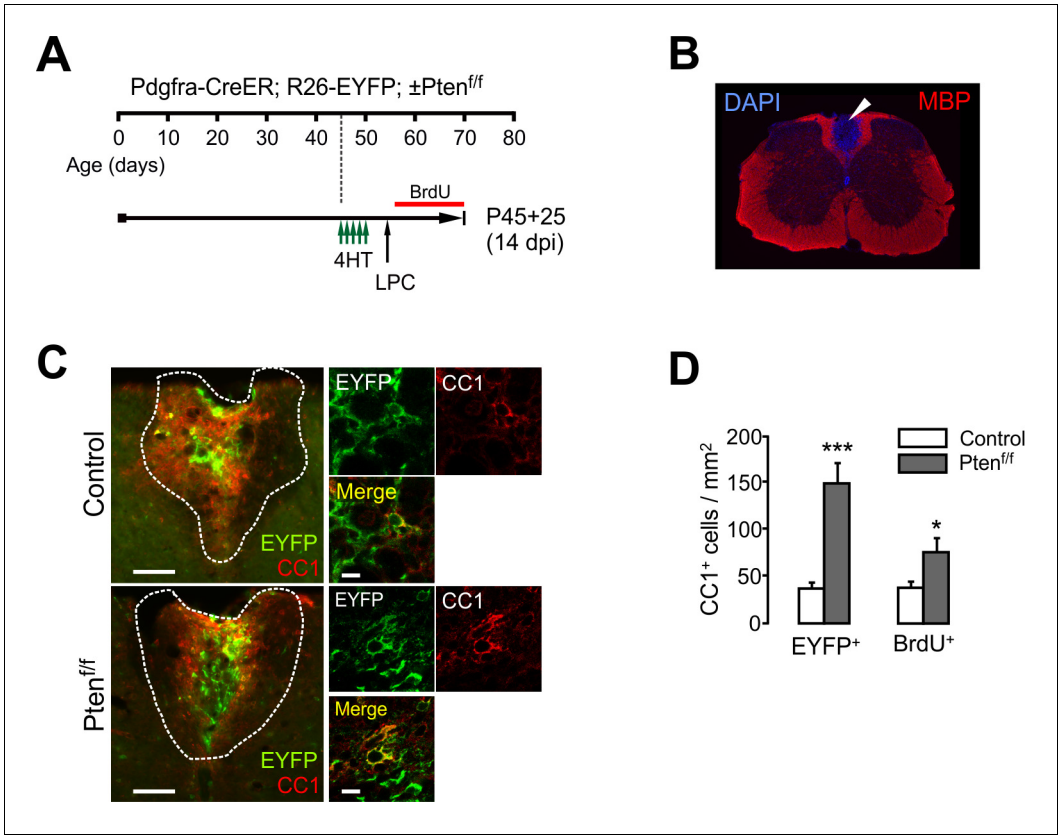

Figure 6—figure supplement 1. OPC-specific *Pten* ablation facilitates oligodendrocyte regeneration after lysolecithin-induced demyelination in the spinal cord. (**A**) Experimental scheme for 4HT, BrdU and LPC injection into *Pdgfra-CreER; R26-EYFP; ±Pten$^{f/f}$* mice, and for mouse sampling. Five injections of 4HT (1 mg per injection) were given between P45 and P47, and LPC was injected at P55. BrdU was administered from P56 to the sampling age only via drinking water. (**B**) Loss of MBP immunoreactivity (arrowhead) at an LPC-injected area in the SC dorsal WM. (**C**) Fluorescence (left) and confocal images (right) of the SC dorsal WM at 14 dpi. Scale bars, 100 μm (left) and 10 μm (right). (**D**) Quantification of newly generated EYFP^{+}CC1^{+} OLs (left) and BrdU^{+}CC1^{+} cells (right). Data are represented as mean ±S.E.M. n = 3 mice per group. *p<0.05; ***p<0.001. Unpaired Student's t-test. The numerical data for the graphs are available in ***Figure 6—figure supplement 1—source data 1***.

DOI: https://doi.org/10.7554/eLife.32021.021

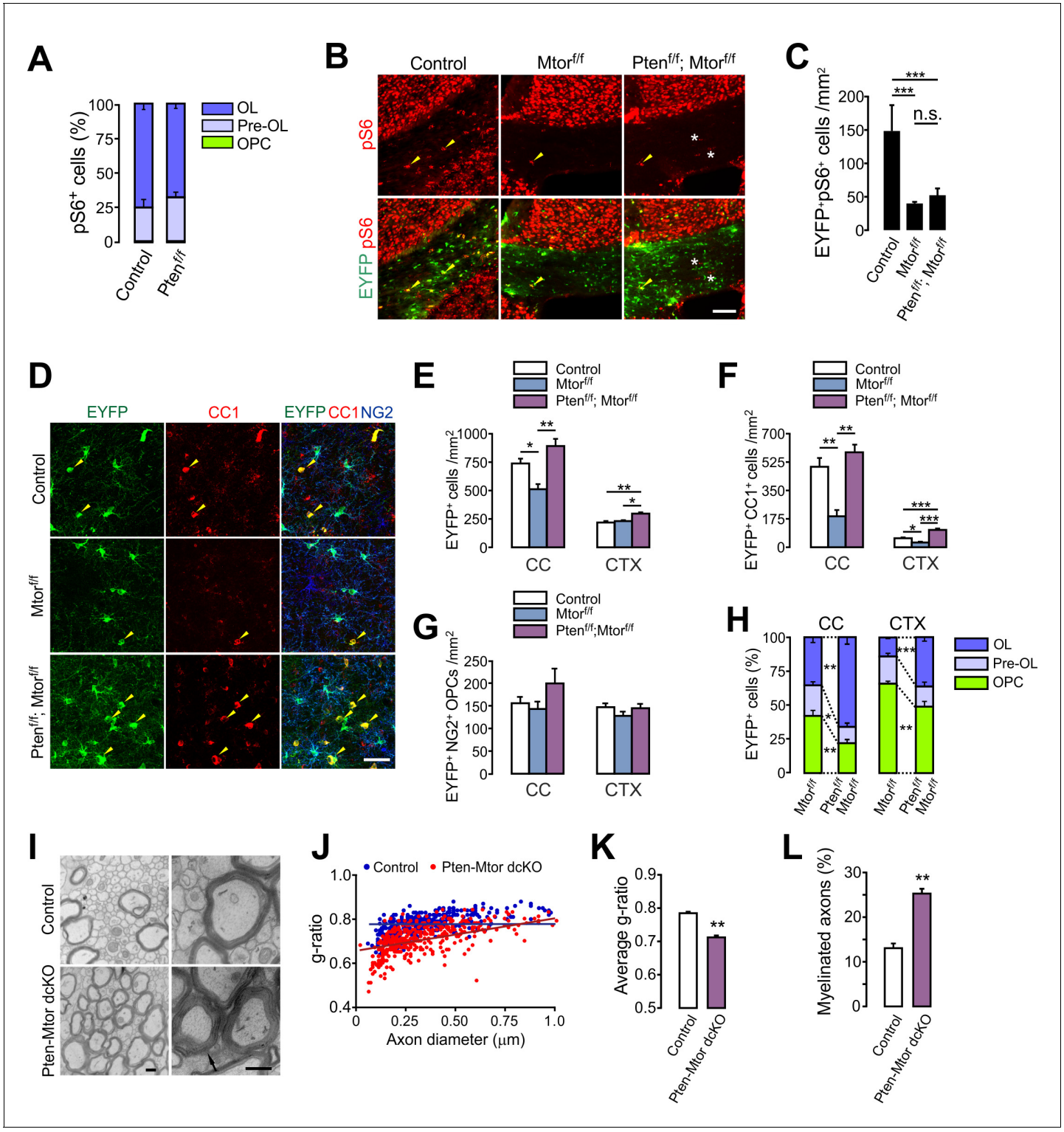

Figure 7. mTOR is dispensable for the enhanced oligodendrocyte generation from PTEN-deficient OPCs and the subsequent hypermyelination. (**A**) Percentage of OPC, pre-OL and OL among EYFP$^+$pS6$^+$ cells in the CC of the control (*Pdgfra-CreER; R26-EYFP*) and *Pten* cKO (*Pdgfra-CreER; R26-EYFP; Pten$^{f/f}$*) mice (P20 +21). Almost all pS6 immunoreactivities were observed either in EYFP$^+$NG2$^-$ pre-OLs or in EYFP$^+$CC1$^+$ OLs, but not in NG2$^+$ OPCs. More than 150 callosal EYFP$^+$pS6$^+$ cells were analyzed per mouse. n = 4 mice per group. (**B**) Validation of effective mTOR inactivation with pS6 immunofluorescence in OPC-specific *Mtor* and *Pten-Mtor* double cKO mice (*Pdgfra-CreER; R26-EYFP; ±Pten$^{f/f}$; ±Mtor$^{f/f}$*, P20 +21). Arrowheads and asterisks indicate pS6$^+$EYFP$^+$ and pS6$^+$EYFP$^-$ cells, respectively. Scale bar, 100 μm. (**C**) Quantification of the EYFP$^+$pS6$^+$ cells in the CC. n = 3 mice per

Figure 7 continued on next page

Figure 7 continued

group. (**D**) Confocal images of EYFP$^+$ cells in the CTX showing their maturation stage. Arrowheads indicate newly differentiated EYFP$^+$CC1$^+$ OLs. Scale bar, 50 µm. (**E - G**) Quantification of total EYFP$^+$ cells (**E**), EYFP$^+$CC1$^+$ OLs (**F**), and EYFP$^+$NG2$^+$ OPCs (**G**) in the CC. (**H**) Percentages of OPC, pre-OL and OL among EYFP-labeled cells of *Mtor* cKO and *Pten-Mtor* cKO mice (P20 +21). (**I**) Representative EM of callosal axons in the control (*Pten*$^{f/f}$) and *Pten-Mtor* cKO mice (P13 +17). An arrow indicates altered myelin thickness. Scale bar, 500 nm. (**J**) Scatter plot of individual *g*-ratios. (**K**) Average of *g*-ratios. At least 130 axons per mouse, and three mice per group were analyzed. (**L**) Percentage of myelinated axons. Data are represented as mean ±S.E.M. n = 6 (control), 4 (*Mtor* cKO), or 4 (*Pten-Mtor* cKO) mice for (E - H), n = 3 mice per group for (I - L). *p<0.05; **p<0.01; ***p<0.001. One-way ANOVA with Bonferroni test for (C, E – G). Unpaired Student's *t*-test for (**H, K, L**). The numerical data for the graphs are available in ***Figure 7—source data 1***.
DOI: https://doi.org/10.7554/eLife.32021.024

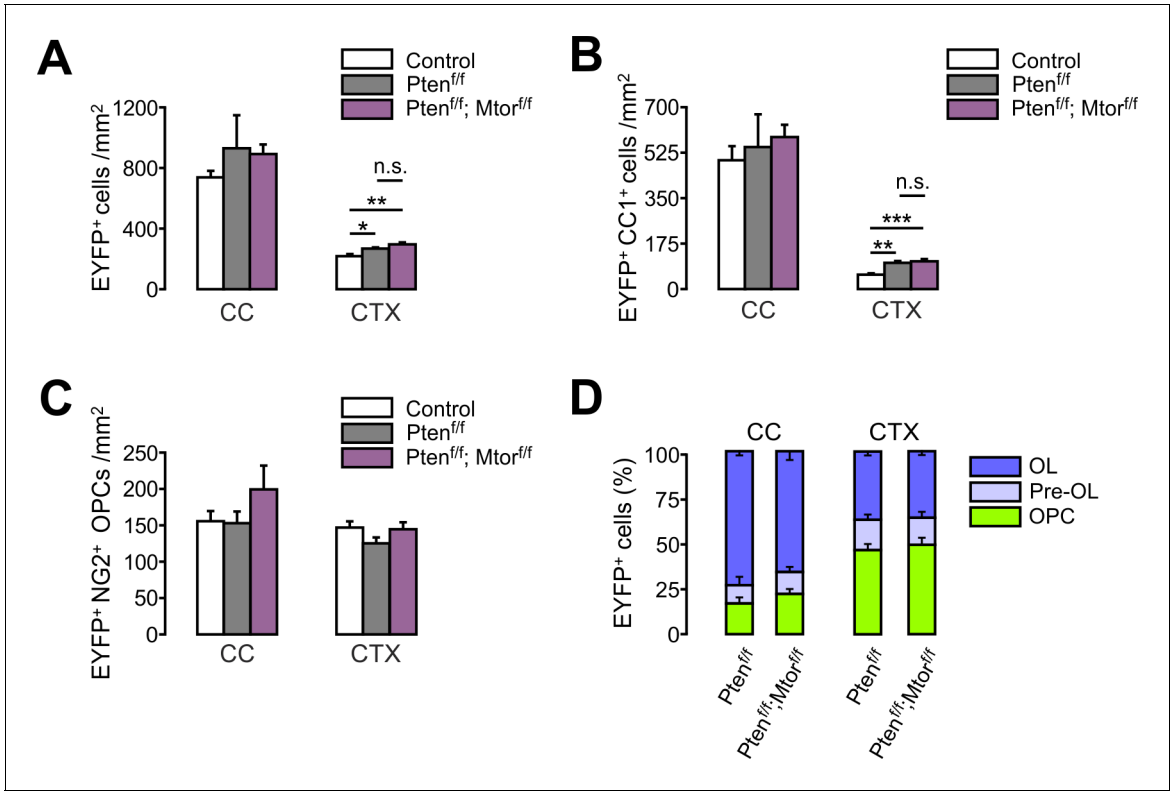

Figure 7—figure supplement 1. Additional *Mtor* ablation does not reverse *Pten*-ablation-induced oligodendrocyte promotion in the brain. (**A**) Quantification of EYFP$^+$ cells in the control (*Pdgfra-CreER; R26-EYFP*), *Pten* cKO, and *Pten-Mtor* double cKO mice (P20 +21). (**B, C**) Quantification of EYFP$^+$CC1$^+$ OLs (**B**) and EYFP$^+$NG2$^+$ OPCs (**C**). (**D**) Percentages of OPC, pre-OL, and OL among EYFP-labeled cells. Data are represented as mean ±S.E.M. n = 4 (control and *Pten-Mtor* double cKO) or 5 (*Pten* cKO) mice. One-way ANOVA with Bonferroni post hoc test for (A - C), and unpaired Student's t-test for (**D**). The numerical data for the graphs are available in ***Figure 7—figure supplement 1—source data 1***.

DOI: https://doi.org/10.7554/eLife.32021.025

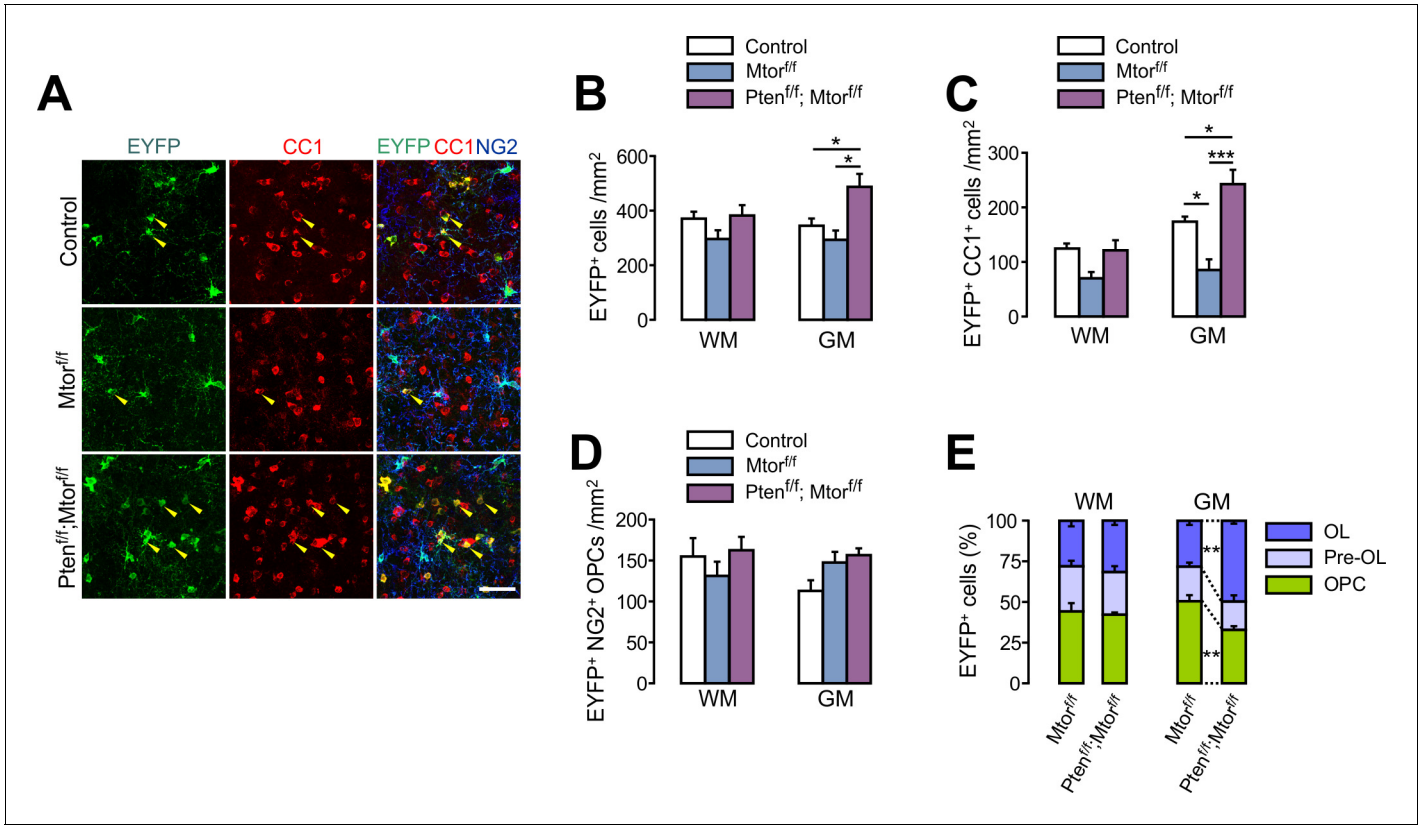

Figure 7—figure supplement 2. Additional *Pten* ablation restores oligodendrocyte differentiation in the spinal cord of *Mtor* cKO mice. (**A**) Confocal images of EYFP$^+$ cells in the GM-SC of the control (*Pdgfra-CreER; R26-EYFP*), *Mtor* cKO, and *Pten-Mtor* double cKO mice. Arrowheads indicate newly generated EYFP$^+$CC1$^+$ OLs. Scale bar, 50 µm. (**B - D**) Quantification of EYFP$^+$ cells (**B**), EYFP$^+$ CC1$^+$ OLs (**C**), and EYFP$^+$NG2$^+$ OPCs (**D**) in the SC of control, *Mtor* cKO, and *Pten-Mtor* double cKO mice. (**E**) Percentages of OPC, pre-OL, and OL among EYFP-labeled cells in the SC of *Mtor* cKO and *Pten-Mtor* double cKO mice. Data are represented as mean ±S.E.M. n = 6 (control) or 4 (*Mtor* cKO and *Pten-Mtor* cKO) mice. One-way ANOVA with Bonferroni test for (**B - D**). Unpaired Student's t-test for (**E**). *p<0.05, **p<0.01, ***p<0.001. The numerical data for the graphs are available in ***Figure 7—figure supplement 2—source data 1***.

DOI: https://doi.org/10.7554/eLife.32021.027

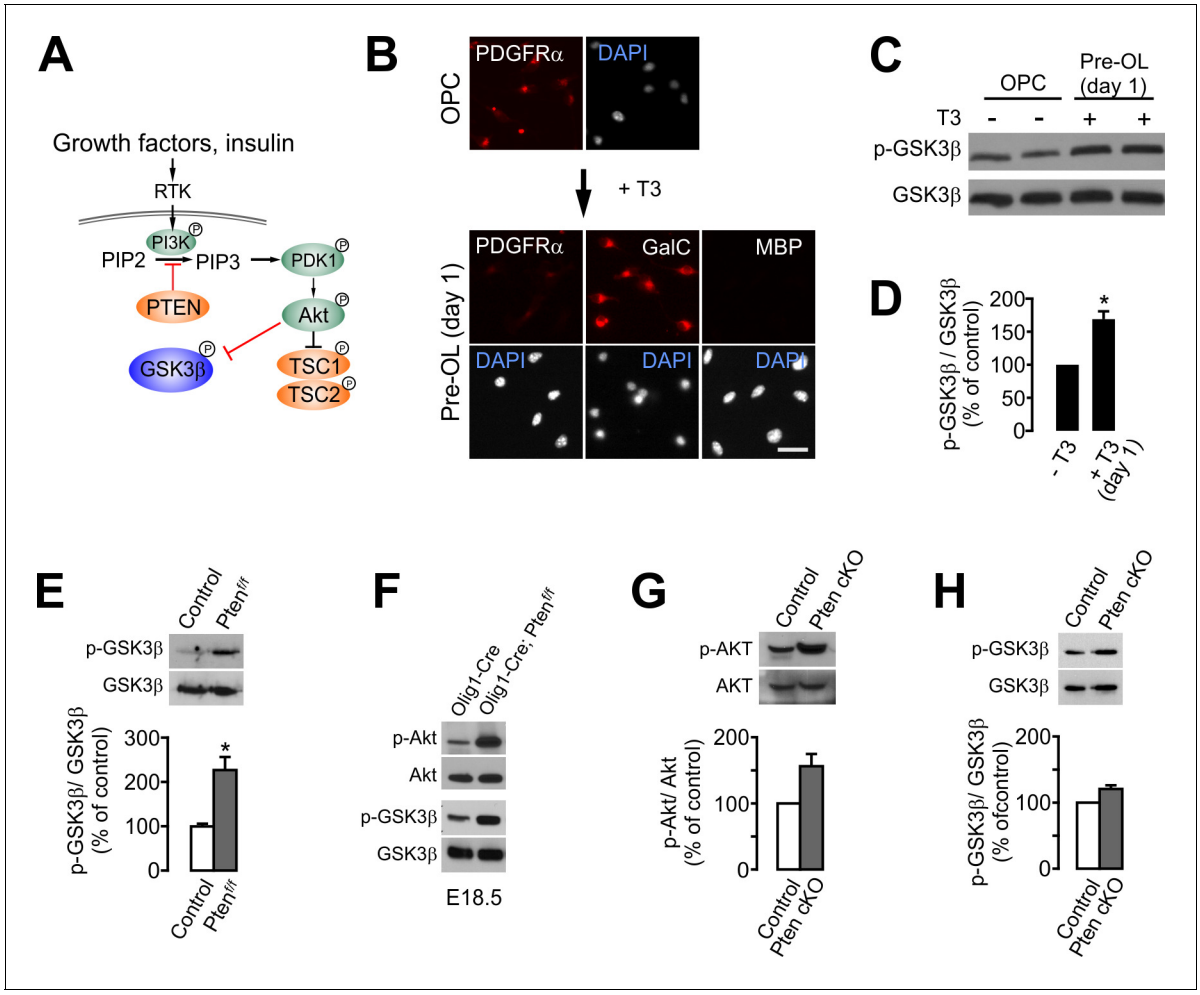

Figure 8. OPC-specific *Pten* ablation enhances the inhibitory phosphorylation (Ser9) of GSK3*β*. (**A**) Schematic diagram for the signaling flow of PTEN-Akt-GSK3*β*. (**B**) *In vitro* OL differentiation from OPCs with T3. One day after T3 addition, the majority of cells become pre-OLs expressing GalC, but not MBP. Scale bar, 20 μm. (**C**) Western blot analysis for phospho-GSK3*β* (p-GSK3β^{Ser9}) levels with oligodendroglial primary culture (with or without T3 incubation for 1 day). (**D**) Quantification of p-GSK3β^{Ser9} levels. n = 3 independent replicates. (**E**) Western blot and quantification of p-GSK3*β* levels in the EYFP^{+} cells obtained from *Pdgfra-CreER; R26-EYFP;* ±*Pten*$^{f/f}$ mice (P20 +21) by FACS. n = 3 mice per group. (**F**) Western blot of the cortical lysates of *Olig1-Cre* (control) and *Olig1-Cre; Pten*$^{f/f}$ embryo (E18.5). n = 1 mouse per group. (**G, H**) Western blot analyses and quantification of the levels of p-Akt^{Ser473} (**G**) and p-GSK3β^{Ser9} (**H**) in *Pten*-deleted OPCs *in vitro*. OPC primary culture was obtained from 4HT-administered *Pten*$^{f/f}$ (control) or *Pdgfra-CreER; Pten*$^{f/f}$ (*Pten* cKO) pups (P1 +1). n = 3 for (**G, H**) independent replicates. Data are represented as mean ±S.E.M. *p<0.05. Paired Student's t-test for (**D, G, H**). Unpaired Student's *t*-test for (**E**). The numerical data for the graphs are available in ***Figure 8—source data 1***. Original western images are available in ***Figure 8—source data 2***.

DOI: https://doi.org/10.7554/eLife.32021.030

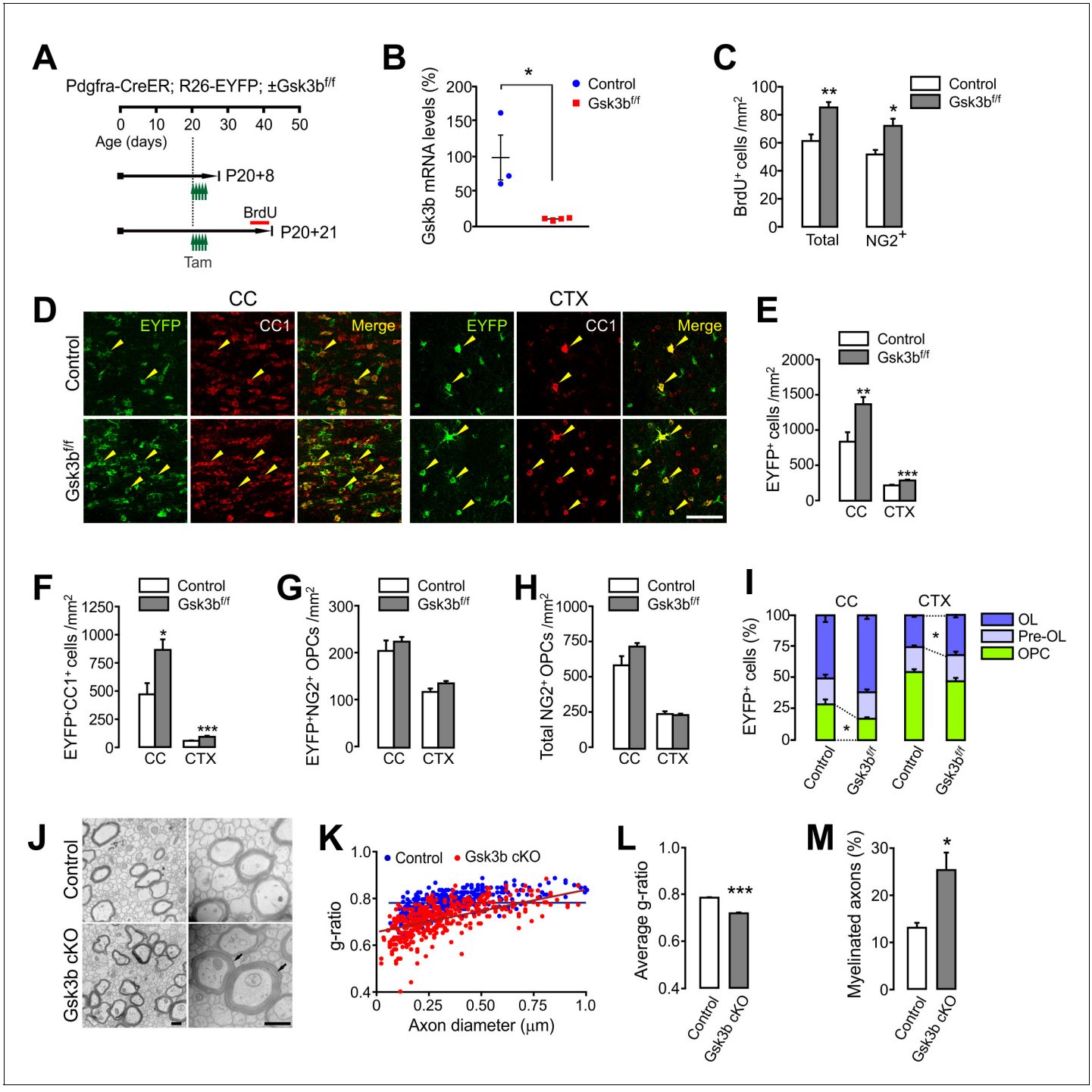

Figure 9. OPC-specific Gsk3b ablation enhances oligodendrocyte differentiation in the brain. (**A**) Experimental scheme for tamoxifen and BrdU administration into *Pdgfra-CreER; R26-EYFP; ±Gsk3b$^{f/f}$* and for mouse sampling. Tamoxifen (40 mg/kg per i.p. injection) was injected five times for 2.5 days starting P20. (**B**) Validation of *Gsk3b* deletion. EYFP^{+} cells were isolated from the CTX of *Pdgfra-CreER; R26-EYFP; ±Gsk3b$^{f/f}$* mice by FACS at P20 +8. The isolated EYFP-labeled cells were subjected to RT-qPCR for *Gsk3b* mRNA levels. n = 3 (control) and 4 (*Gsk3b* cKO) mice. (**C**) Quantification of BrdU^{+} cells in the CTX at P20 +21. There was an increases in BrdU^{+}NG2^{+} OPCs in the *Gsk3b* cKO mice (P20 +21). n = 5 mice per group. (**D**) Confocal images of EYFP^{+}CC1^{+} OLs (arrowheads) in the CC and CTX. Scale bar, 50 µm. (E - H) Quantification of total EYFP^{+} cells (**E**), EYFP^{+}CC1^{+} OLs (**F**), EYFP^{+}NG2^{+} OPCs (**G**), and total NG2^{+} OPCs (**H**). (**I**) Percentages of OPC, pre-OL and OL among EYFP-labeled cells. n = 8 (control) or 6 (*Gsk3b* cKO) mice for (E – I). (**J**) Representative EM of callosal axons (P13 +17). *R26-EYFP* (control) or *Pdgfra-CreER; R26-EYFP; Gsk3b$^{f/f}$* (*Gsk3b* cKO) mice were used. Scale bar, 500 nm. (**K**) Scatter plot of the g-ratios. (**L**) Average of g-ratio. At least 130 axons per mouse, three mice per group were analyzed. (**M**)

Figure 9 continued on next page

Figure 9 continued

Percentage of myelinated axons. Data are represented as mean ±S.E.M. n = 3 mice per group (K – M). *p<0.05; **p<0.01; ***p<0.001. Unpaired Student's t-test. The numerical data for the graphs are available in ***Figure 9—source data 1***.

DOI: https://doi.org/10.7554/eLife.32021.033

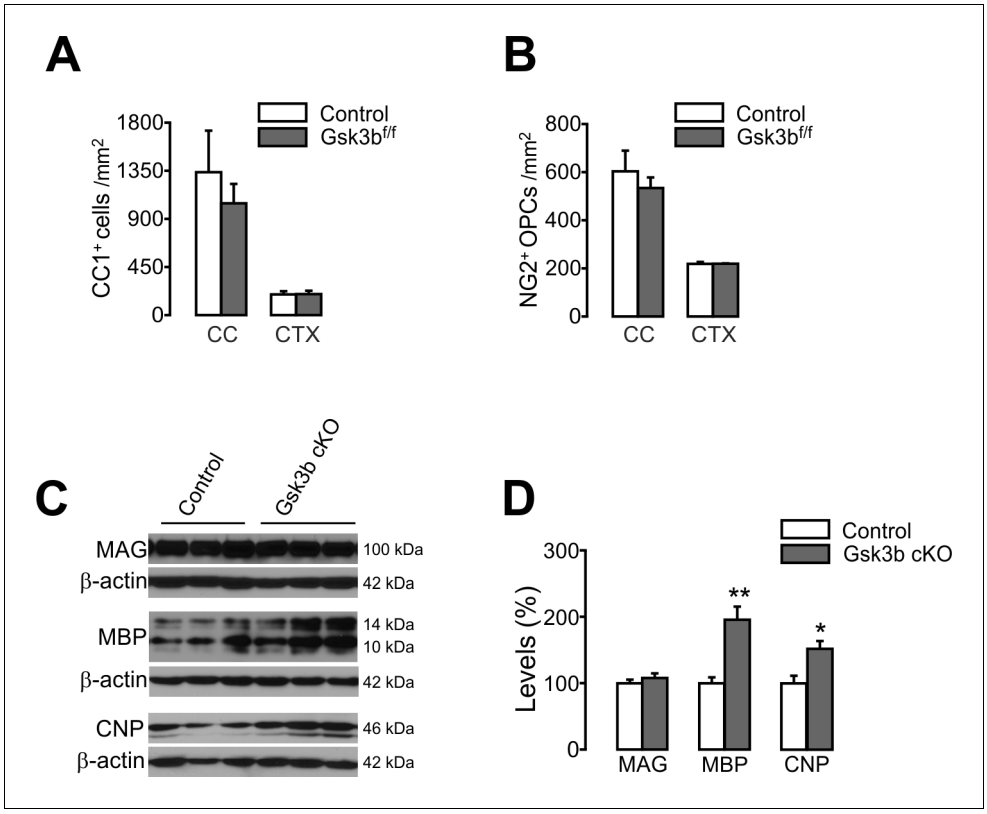

Figure 9—figure supplement 1. OL-specific *Gsk3b* ablation does not change the number of oligodendrocyte, but enhances expression levels of MBP and CNP. (**A**) Quantification of $CC1^+$ OLs in the CTX of the control (*Mog-iCre; R26-EYFP*) and OL-specific *Gsk3b* cKO (*Mog-iCre; R26-EYFP; Gsk3b$^{f/f}$*) mice at P31. (**B**) Quantification of $NG2^+$ OPCs. n = 3 mice per group for (**A, B**). (**C, D**) Western blot analysis of cortical lysates for myelin proteins, MAG, MBP, and CNP. Cortices were isolated from *Gsk3b$^{f/f}$* (control) and *Mog-iCre; Gsk3b$^{f/f}$* (*Gsk3b* cKO) mice (**P31**). n = 4 mice per group for (**C, D**). Data are represented as mean ±S.E.M. *p<0.05, **p<0.01. Unpaired Student's t-test. The numerical data for the graphs are available in ***Figure 9—figure supplement 1—source data 1***. Original western images are available in ***Figure 9—figure supplement 1—source data 2***. List of source data files.

DOI: https://doi.org/10.7554/eLife.32021.034